Journal of Environmental Management 246 (2019) 63–70

Contents lists available at ScienceDirect

Journal of Environmental Management

journal homepage: www.elsevier.com/locate/jenvman

Research article

Non-thermal plasma needle as an effective tool in dimethoate removal from water

Tatjana Mitrović[a], Saša Lazović[b], Branislav Nastasijević[c], Igor A. Pašti[d], Vesna Vasić[c], Tamara Lazarević-Pašti[c,*]

[a] The Jaroslav Cerni Institute for the Development of Water Resources, Jaroslava Cernog 80, Belgrade, Serbia
[b] Institute of Physics, University of Belgrade, Pregrevica 118, 11080, Belgrade, Serbia
[c] Department of Physical Chemistry, Vinča Institute of Nuclear Sciences, University of Belgrade, Mike Petrovića Alasa 12-14, P. O. Box 522, 11001, Belgrade, Serbia
[d] University of Belgrade, Faculty of Physical Chemistry, Studentski Trg 12-16, 11158, Belgrade, Serbia

ARTICLE INFO

Keywords:
Dimethoate
Omethoate
Organophosphate pesticides
Non-thermal plasma
Plasma needle
Degradation

ABSTRACT

Intensive use of pesticides requires innovative approaches for their removal from the environment. Here we report the method for degradation of dimethoate in water using non-thermal plasma needle and analyze kinetics of dimethoate removal and possible degradation pathways. The effects of dimethoate initial concentration, plasma treatment time, Argon flow rate and the presence of radical promoters on the effectiveness of proposed method are evaluated. With argon flow rate of 0.5 slm (standard litres *per* minute) 1×10^{-4} M dimethoate can be removed within 30 min of treatment. Using UPLC analysis it was confirmed that one of the decomposition products is dimethoate oxo-analogue omethoate, which is in fact more toxic than dimethoate. However, the overall toxicity of contaminated water was reduced upon the treatment. The addition of H_2O_2 as a free radical promoter enhances dimethoate removal, while $K_2S_2O_8$ results with selective conversion to omethoate. Using mass spectrometry in combination with the theoretical calculations, possible degradation pathways were proposed. The feasibility of the proposed method for dimethoate degradation in real water samples is confirmed. The proposed method is demonstrated as a highly effective approach for dimethoate removal without significant accumulation of undesirable toxic products and secondary waste.

1. Introduction

Organophosphorus pesticides (OPs) have been used globally since the first introduction of a synthetic insecticide parathion for crop protection in 1944 (Liu et al., 2001). Their high stability, environmental endurance, poor biodegradability and expansive usage led to the pesticide accumulation in our environment, particularly in water (Manoli et al., 2018). OPs are toxic to humans and most animals due to the inhibition of the enzymes acetylcholinesterase (AChE) (Colovic et al., 2013) which leads to acetylcholine accumulation, resulting in disrupted neurotransmission (Lazarevic-Pasti et al., 2017).

Dimethoate (DMT, Fig. 1) is very powerful pesticide and has harmful effects on the health of humans and animals because of its toxicity even at low concentrations (liver, endocrine organs, lymphatic system, chronic renal disease, parathyroid hyperplasia, oxidative stress, DNA damage in rainbow trout, and a skin irritant). World Health Organization classified it as "moderately hazardous" with a guideline value of 6 μg/l in drinking water (WHO, 2011). However, upon oxidation, dimethoate transforms to omethoate (OMT, Fig. 1), its oxo-analogue, which is more toxic than DMT (Lazarevic-Pasti et al., 2016). Omethoate could also be found in the environment, due to the presence of various oxidizing agents (Lazarevic-Pasti et al., 2016). Therefore, systematic work is needed to develop new methods for DMT and OMT quantification (Cui et al., 2018; Lazarevic-Pasti et al., 2010) and efficient routes for complete degradation of dimethoate, its by-products and the reduction of its toxic effects (Lazarevic-Pasti et al., 2016, 2018; Mirkovic et al., 2016).

Difference approaches for OP removal from the environment have been developed so far. Well-known methods include degradation (chemical or microbial) or adsorption on different types of materials. Advanced Oxidation Process (AOPs) such as Fenton oxidation (Badawy et al., 2006), photocatalysis (Savic et al., 2019; Wu and Linden, 2010),

* Corresponding author. Department of Physical Chemistry, Vinča Institute of Nuclear Sciences, University of Belgrade, Mike Petrovića Alasa 12-14, P. O. Box 522, 11001, Belgrade, Serbia.
E-mail addresses: tatjana.mitrovic@jcerni.rs (T. Mitrović), lazovic@ipb.ac.rs (S. Lazović), branislav@vin.bg.ac.rs (B. Nastasijević), evasic@vin.bg.ac.rs (I.A. Pašti), igor@ffh.bg.ac.rs (V. Vasić), tamara@vin.bg.ac.rs, lazarevictlj@yahoo.com (T. Lazarević-Pašti).

https://doi.org/10.1016/j.jenvman.2019.05.143
Received 29 January 2019; Received in revised form 14 May 2019; Accepted 28 May 2019
Available online 04 June 2019

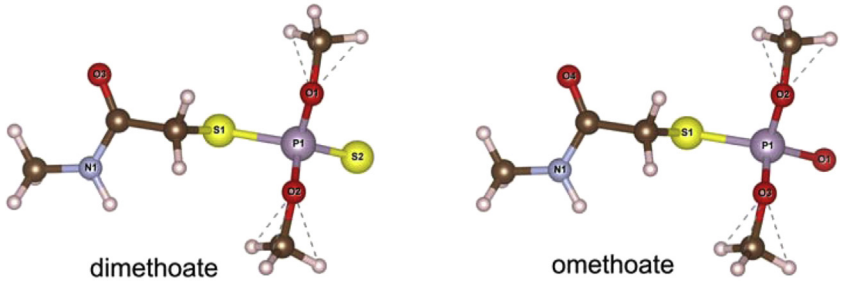

Fig. 1. The structures of dimethoate and its oxo-analogue omethoate. Observed that S2 atom of dimethoate is replaced by the O atom (denoted as O1 in omethoate structure). Graphical presentation of molecular structures is made using the code VESTA (Momma and Izumi, 2008).

ozonation (Matsushita et al., 2018), and electrochemical degradation (Samet et al., 2010) are being outlined by many authors as suitable for pesticide removal. On the other hand, pesticide removal by adsorption was demonstrated for different materials, like mesoporous monetite (Mirkovic et al., 2016), porous metal – organic frameworks (Zhu et al., 2015), mineral surfaces (Leovac et al., 2015), organohydrotalcite (Bruna et al., 2006), activated carbon and zeolites (Valickova et al., 2013), carbon-based materials (Lazarevic-Pasti et al., 2016; Matsushita et al., 2018), materials from graphene family (Lazarevic-Pasti et al., 2018) and others. Nevertheless, these approaches suffer from both poor degradation efficiency and formation of very toxic by-products or formation of secondary waste (used adsorbents contaminated with pesticides) which have to be additionally treated.

Plasma oxidation has been confirmed as very effective method for decomposition which avoids the formation of undesirable secondary polluted waste (Hu et al., 2013; Yang and Tezuka, 2011). Depending on electron temperature, plasma can be thermal (plasma components in thermal equilibrium) or non-thermal (NTP). In NTP the electrons are at much higher temperature (10^4 K) than the heavy particles, ions and neutrals (temperatures as low as the room temperature). As they collide with gas molecules chemically reactive species are being generated (Jiang et al., 2016). Because in NTPs chemically reactive species can be abundantly produced at low temperatures overheating can be mitigated and sensitive samples can be safely treated (Lazovic et al., 2010) even at atmospheric pressure (Maletic et al., 2012). Chemical conditions that occur in electrical discharges in water include the direct formation of reactive species such as •OH, •O, •H radicals, H_2O_2, and O_3 (Puac et al., 2014). UV emission generated from NTPs also further improves oxidation efficiency. As a result, a combination of physical and chemical processes is very convenient for degradation of very complex and resistant pollutants (Badawy et al., 2006).

Many hazardous organic compounds are readily attacked by excited species, free radicals, electrons, ions and/or UV photons generated in NTP resulting with formation of small organic and inorganic molecules (Lou et al., 2012). Moreover, by using plasma generation devices, oxidant radical species can be formed directly in water (Foster et al., 2012), at the vicinity of its surface (Kanazawa et al., 2011), or in bubbles injected inside the contaminated solution (Yamatake et al., 2007), what makes them promising techniques for water treatment. However, while plasma treatment seems as promising route for OPs removal from water, NTP degradation pathways are still not well understood.

In this contribution we investigate the novel method for dimethoate removal from water using non-thermal plasma needle. The plasma needle is a type of non-thermal atmospheric plasma. It is a novel design of a plasma source capable of generating abundance of chemically very reactive species with low powers consumption (few Watts). It operates at atmospheric pressure producing well localized plasma at the tip of the powered electrode. Samples treated with plasma needle are not overheated and typically their temperature is increased only for a few degrees at most. The aim of the present work is to investigate DMT removal from water using non-thermal plasma needle treatment and to address all the critical points of such approach – from the understanding of the optimal conditions and degradation pathways to possible application in real samples. Considering the introduction of a novel method for DMT removal from water, the influence of various parameters, such as DMT initial concentration, plasma treatment time, Argon flow rate and the presence of radical promoters on DMT removal efficiency is addressed in details. Different kinetic parameters are evaluated and discussed in order to determine optimal conditions for DMT removal. In order to contribute the understanding of DMT degradation, possible pathways are proposed. Moreover, we estimate the toxicity of dimethoate samples before and after the treatment with non-thermal plasma needle. Additionally, the feasibility of proposed method was demonstrated for real samples.

2. Materials and methods

2.1. Chemicals

AChE (specific activity 288 IU/mg solid, 408 IU/mg protein) from electric eel, H_2O_2, $K_2S_2O_8$, acethylthiocholine iodide (ASChI) and 5,50-dithio-bis-(2-nitrobenzoic acid) (DTNB) were purchased from Sigma Aldrich (St. Louis, MO, USA). The pesticides (at least 93% purity) dimethoate and omethoate were purchased from Pestanal, Sigma Aldrich, Denmark. The pesticide working solutions were prepared by dilution of the 1×10^{-1} M stock solutions in ethanol. The final working solutions contained maximal 2% ethanol. The pesticide stock solutions were held in refrigerator until used. All chemicals were used without further purification. Deionised water was used throughout.

2.2. Plasma treatment of dimethoate

Plasma needle operating at 25 kHz was used for all treatments. Characterization of the plasma device has been presented earlier in details (Zaplotnik et al., 2015). DMT solutions (10 ml) of various concentrations (1×10^{-3} M, 1×10^{-4} M and 1×10^{-5} M) were placed in 50 ml glasses and exposed to plasma (Fig. 2). Argon was used as a feed gas (0.5–2 standard liter *per* minute (slm) flow rate). Power supply provided 2.5 kV (root mean square value). The tip of the powered electrode was placed 5 mm below the surface of the samples. The exposure time was varied from 1 to 120 min.

2.3. Analysis methods

2.3.1. UPLC analysis

Waters ACQUITY Ultra Performance Liquid Chromatography (UPLC) system coupled with a tunable UV detector controlled by the Empower software was used. Chromatographic separations were run on an ACQUITY UPLC™ BEH C18 column with the dimensions 1.7 µm, 100 mm × 2.1 mm (Waters). The analyses of dimethoate and omethoate solutions were done under isocratic conditions with mobile phase consisting of 10% acetonitrile and 90% water (v/v). The eluent flow rate was 0.2 mL min^{-1} and the injection volume was 10 µL.

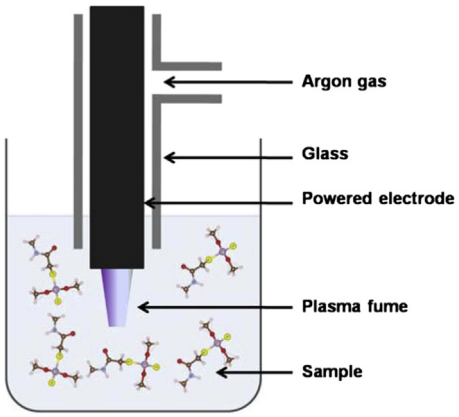

Fig. 2. Schematic representation of non-thermal plasma needle treatment of dimethoate solutions.

Optical detection of dimethoate and omethoate was done at 200 nm. Under described conditions retention times of dimethoate and omethoate were 1.73 ± 0.05 min and 1.07 ± 0.05 min, respectively.

2.3.2. Mass spectrometry analysis (MS)

The qualitative analysis of intermediates and products during non-thermal plasma degradation of dimethoate was performed using Quattro Micro Mass Spectrometer with a Z-spray interface. The sample solutions were introduced into an ESI source with a syringe pump at a flow rate of 15 μL/min. Acquisition of data was done using MassLynx NT software version 4.1., in ESI scan mode (positive polarity) with the mass range from 50 to 300 Da and mass resolution of 0.5 Da. Scan time was set at 0.3 s, inter scan time was 0.1 s, and run duration was 1 min. The optimized instrument settings used for the ionization are shown in Table S1 (Supplementary Information). Stock solution of dimethoate standard was made in deionised water in a concentration of 10^{-1} M. Samples used for MS analysis (scanning) were diluted with 0.1% formic acid in methanol and with 5 mM ammonium formate buffer (pH 5) to a final concentration of 10^{-3} M (standard solution).

2.4. Toxicity measurements

AChE inhibition measurements were performed to quantify toxicity of dimethoate and also to investigate if there is a transformation of dimethoate into omethoate, which is much more toxic than corresponding thio-form (Lazarevic-Pasti et al., 2016). Oxo-form of OP can reveal toxic effects at the concentrations which are below detection limits of UPLC but could be observed using AChE inhibition measurements. AChE activity was assayed according to Ellman's procedure (Ellman et al., 1961). The procedure is described in detail in Ref (Lazarevic-Pasti et al., 2016) and here we provide it for the sake of completeness. The *in vitro* experiments were performed by exposure of 2.5 IU commercially purified AChE from electric eel to OP solutions obtained in adsorption experiments at 37 °C in 50 mM PB pH 8.0 (final volume 0.650 mL). The enzymatic reaction was started by the addition of acetylcholine-iodide (AChI) in combination with 5,5′-Dithiobis(2-nitrobenzoic acid) (DTNB) as a chromogenic reagent, and allowed to proceed for 8 min until stopped by 10% sodium dodecyl sulphate (SDS). The product of enzymatic reaction, thiocholine, reacts with DTNB and forms 5-thio-2-nitrobenzoate, whose optical adsorption was measured at 412 nm. It should be noted that in these measurements the enzyme concentration was constant and set to give an optimal spectrophotometric signal. Physiological effects were quantified as AChE inhibition given as:

$$\text{AChE inhibition} = 100 \times (A_0 - A)/A_0 \quad (1)$$

where A_0 and A stand for the AChE activity in the absence of OP and the one measured after the exposure to a given OP.

2.5. DFT calculations

The calculations were based on Density Functional Theory (DFT) within the Generalized Gradient Approximation in the parametrization of Perdew, Burke and Ernzerhof (PBE) (Perdew et al., 1996). The calculations were performed using the Quantum ESPRESSO (QE) *ab initio* package (Giannozzi et al., 2009) using ultra soft pseudopotentials. Complete description of computational setup is provided in Supplementary Information.

In order to identify reactive parts of DMT and OMT we calculated Fukui functions proposed by Yang (Yang and Mortier, 1986) defined as:

$$f_k^+ = q_k(N+1) - q_k(N) \quad (2)$$

$$f_k^- = q_k(N) - q_k(N-1) \quad (3)$$

In the equations above $q_k(N+1)$, $q_k(N)$ and $q_k(N-1)$ are the atomic charges of atom k in a given molecule which negatively charges, neutral and positively charged, respectively. Local sites with large values of f_k^- react with electron acceptors, while the sites with a large f_k^+ will react with electron donors.

3. Results and discussion

3.1. Treatment of dimethoate with plasma

Aqueous solutions of 1×10^{-3} M, 1×10^{-4} M and 1×10^{-5} M dimethoate were treated with plasma as described in Section 2.2. The species in the treated samples were identified by chromatographic techniques. DMT and OMT were identified in the sample according the corresponding standards, at the given retention times (Section 2.3.1). The concentration of dimethoate and omethoate in working solutions were measured as the function of the plasma treatment time. Fig. 3 illustrates the results obtained for 1×10^{-3} M and 1×10^{-5} M initial DMT concentrations, i.e. DMT degradation and the corresponding OMT formation and degradation curves at flow rate 0.5 slm.

It is obvious that the concentration of dimethoate decreased with the plasma treatment time. The degradation of dimethoate was followed by the formation of omethoate as the intermediate product, which also undergoes to a complete degradation. The change of the concentration for both compounds *vs.* time is dependent on the treatment time, as well on the plasma flow rate. However, the maximum concentration of a more toxic OMT is achieved significantly faster at a

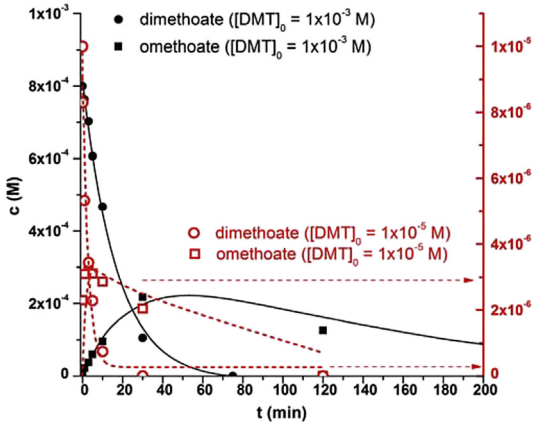

Fig. 3. The change of dimethoate (circles) and omethoate (squares) concentration as the function of plasma treatment time at 0.5 slm Argon flow rate for 1×10^{-3} M (solid) and 1×10^{-5} M (dash) initial dimethoate concentration. The data points represent experimentally obtained results, while the curves were calculated from eqs. (4) and (6), see further.

Table 1
Kinetic parameters of dimethoate degradation and omethoate formation and degradation.

$[DMT]_0$ (M)	Ar flow (slm)	k_{obs} (min^{-1})	k_1 (min^{-1})	k_2 (min^{-1})	[a][OMT] (M)	[b]t_{max} (min)
1×10^{-3}	0.5	5.05×10^{-2}	3.94×10^{-2}	0.80×10^{-2}	3.30×10^{-4}	50.63
	1	5.48×10^{-2}	4.48×10^{-2}	0.75×10^{-2}	3.58×10^{-4}	47.72
	2	7.27×10^{-2}	7.01×10^{-2}	0.79×10^{-2}	3.60×10^{-4}	35.00
1×10^{-4}	0.5	10.3×10^{-2}	8.80×10^{-2}	1.30×10^{-2}	1.65×10^{-5}	26.86
	1	16.69×10^{-2}	16.07×10^{-2}	4.77×10^{-2}	2.18×10^{-5}	10.74
	2	30.95×10^{-2}	20.00×10^{-2}	5.16×10^{-2}	4.20×10^{-5}	9.09
1×10^{-5}	0.5	28.60×10^{-2}	25.70×10^{-2}	2.35×10^{-2}	4.00×10^{-6}	10.23
	1	43.00×10^{-2}	42.85×10^{-2}	2.00×10^{-2}	3.56×10^{-6}	7.50
	2	78.00×10^{-2}	45.20×10^{-2}	6.50×10^{-2}	4.50×10^{-6}	5.02

[a] Maximal OMT concentration (from kinetic analysis).
[b] Time needed to reach the maximal OMT concentration.

lower DMT concentration, and reached the value of about 15–40% of the initial DMT concentration (Table 1).

It is also important to note that the sum of DMT and OMT concentrations *vs*. time is lower compared to the initial DMT concentration before plasma treatment. This fact points out that there are at least two parallel processes of dimethoate degradation induced by plasma treatment, i.e. oxidation to its oxo-form, as well as the hydrolysis by •OH radicals (Hu et al., 2013), which results in DMT degradation, as will be discussed further.

3.1.1. Kinetic parameters

The kinetic traces which follow the decrease of dimethoate concentration fit well to the single exponential decay function, Eq. (4) which is characteristic for pseudo-first order reaction:

$$[DMT] = [DMT]_0 e^{-k_{obs}t} \quad (4)$$

Here, k_{obs} represents the overall observed DMT degradation rate constant, t is the reaction time, while [DMT] and $[DMT]_0$ represent the measured (at a given time of reaction) and the initial DMT concentration. The values k_{obs} were obtained by fitting the experimental data with Eq. (4). On contrary, the change of omethoate concentration *vs.* time is characteristic for series of two first order reactions, illustrated schematically by Eq. (5):

$$DMT \xrightarrow{k_1} OMT \xrightarrow{k_2} products \quad (5)$$

The shape of the curve [OMT] *vs*. time can be described using eq. (6) (Schmid and Sapunov, 1982):

$$[OMT] = \frac{k_1}{k_2 - k_1}[OMT]_0 \cdot \left(e^{-k_1 t} - e^{-k_2 t}\right) \quad (6)$$

where k_1 and k_2 represent rate constants for the first and the second step in Eq. (5). The results presented in Fig. 1 for omethoate suggest that $k_1 \gg k_2$. This fact enabled us to treat the ascending and descending omethoate curves separately, in order to determine k_1 and k_2. In further treatment, the obtained values were included into Eq. (6) in order to recalculate omethoate concentration *vs*. time. The values of rate constants are presented in Table 1, together with the maximal omethoate concentration and time required to reach it. These values were calculated using Eq. (7):

$$t_{max} = \ln \frac{k_1}{k_2} \cdot \frac{1}{(k_1 - k_2)} \quad (7)$$

The results presented as lines in Fig. 3 indicate an excellent fit of the experimental points with calculated values.

Fig. 4 illustrates the changes of DMT degradation constant, k_{obs}, as the function of its initial concentration and the Ar flow rate. It is evident that the degradation rate is significantly decreased with the increasing DMT concentration. However, it increased by increasing the Ar flow rate at a constant DMT concentration. This effect is more pronounced for a lower DMT concentration range. Besides, the time needed to reach

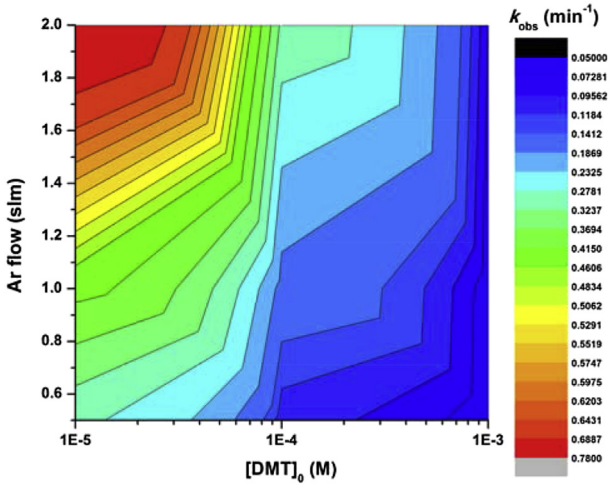

Fig. 4. Dependence of k_{obs} on DMT initial concentration for various flow rates. The rate of DMT degradation is maximized for low DMT concentrations and high Ar flow rates.

the maximal OMT concentration depends also significantly on argon flow rate (Table 1).

The time required to reach the maximum OMT concentration was also concentration and flow rate dependent (Table 1). At the highest level of OMT in all the cases, the DMT concentration decreased below UPLC detection limit. However, the formed OMT induces significant toxicity towards AChE, i.e. the 45%, inhibition of enzyme only at 1×10^{-3} M initial dimethoate, as shown before (Lazarevic-Pasti et al., 2016). Moreover, the concentration of formed OMT at particular DMT concentration increased with the Ar flow rate increasing in all samples.

From everything discussed above, the optimal conditions to achieve the fastest and the most efficient DMT degradation have to be carefully selected, since they depend on the initial DMT concentration and argon flow rate. Also, the time of the treatment plays an important role in these processes. As being measured and modelled using kinetic analysis, the increase of the OMT concentration during the plasma treatment until certain point is inevitable as OMT is intermediate product in dimethoate degradation. It is produced due to the oxidation of the parental DMT in the presence of free radicals formed in water under the influence of plasma radiation. When concerned with the purification of contaminated water, it is important to reduce the DMT concentration, but also to keep the OMT concentration under the limit of toxicity (Lazarevic-Pasti et al., 2016). The applied experimental condition suggest that the argon flow rate of 0.5 slm and 30 min of treatment are the parameters of choice in order to accomplish the best economical aspect of the method, which is also very important. Under these conditions it is possible to successfully remediate DMT from water in the concentration as high as 1×10^{-4} M, which is much more than it can

usually be found in real samples.

The efficiency of proposed method is comparable or better than that of other methods proposed in literature for DMT removal. Namely, there are several methods for dimethoate removal, but these suggest rather long time for its degradation. This significantly impacts the economical benefits of the process. In the case of photocatalytic degradation of dimethoate in the presence of TiO_2 reported by Vela et al. (2018), the time required for 90% pesticide degradation is around 250 min. Moreover, Liu et al. reported that several days are required for complete degradation of DMT using TiO_2/Ce hydrosol-mediated solar photodegradation (Liu et al., 2018). Li et al. recently proposed a method for photocatalytic degradation of dimethoate using mesoporous material TiO2/SBA-15 and solar light (Li et al., 2018). They reported 94% dimethoate degradation after 7 h of treatment. While the efficiency of this approach is high, the method we proposed is much faster, since we achieved 100% removal for 1×10^{-4} M dimethoate after only 30 min. Even though TiO2/SBA-15 used for DMT degradation maintained high photocatalytic activity and good stability during four cycles, plasma needle degradation is a process without any waste, which is extremely important having in mind environmental pollution and the economical aspects of waste recycling. Moreover, it can be performed continuously without interruptions as long as Ar supply is uninterrupted. Moreover, Li et al. (2018) did not consider this method from the aspect of the toxicity of treated samples, so it cannot be claimed that there is no DMT oxidation during this process. On the other hand, we have managed to achieve acceptable levels of OMT during DMT plasma treatment, which was also reflected by toxicity measurements (see further).

3.2. Treatment of dimethoate with plasma in the presence of free radical promoters

The results presented above showed that the plasma treatment of 1×10^{-3} M DMT results in its complete degradation within 80 min. However, a significant amount of more toxic OMT was present even after 120 min of plasma treatment. In order to improve the degradation efficiency, free radical promoters (H_2O_2 and $K_2S_2O_8$) were added to the sample solution. The motivation for the use of free radical promoters is justified below.

The non-thermal plasma is known to produce significant quantities of hydroxyl radical (·OH) and hydrogen peroxide (H_2O_2) (Lou et al., 2012). Hydroxyl radical has a higher standard electrode potential (E° = 2.73 V, and formal potential of 2.31 V at pH = 7 (Armstrong et al., 2013) than H_2O_2 (E° = 1.78 V) (Vanysek, 2005). It is known that species with higher redox potentials are more active in the degradation of organic molecules. In addition, hydrogen peroxide is a source of hydroxyl radicals under UV irradiation (Baxendale and Wilson, 1957). Therefore, we presumed that the addition of H_2O_2 enhances additional formation of · which should make the degradation of DMT even more effective. In additions, many recent studies have investigated the persulfate ability to degrade organic pollutants (Matzek and Carter, 2016). Being stable at ambient temperature, persulfate can be activated by metal reactions or by supplying energy (heat, UV, etc.). The energy supply results in cleavage of the peroxide bond of the persulfate molecule allows the formation of sulphate radicals ($\cdot SO_4^-$). *In situ* formed sulphate radicals have high standard electrode potential between 2.43 V (Armstrong et al., 2013) and 2.6 V (Połczyński et al., 2013), and at nearly neutral pH sulphate radicals are even more potent oxidants than ·OH (Armstrong et al., 2013). Heat-activated persulfate degradation was studied on numerous organic compounds (Chen et al., 2017; Fan et al., 2015; Ji et al., 2015), including OPs (Aimer et al., 2019). Hence, the application of NTP-activated persulfate for similar purposes seems as straightforward.

The DMT solution (1×10^{-3} M, 10 ml) was treated with plasma in the presence of 0.09 M H_2O_2 or $K_2S_2O_8$ for 1, 3, 5, 10 and 30 min with the Argon flow rate of 0.5 slm, under the conditions described in Section 2.2. The results are presented in Fig. 5.

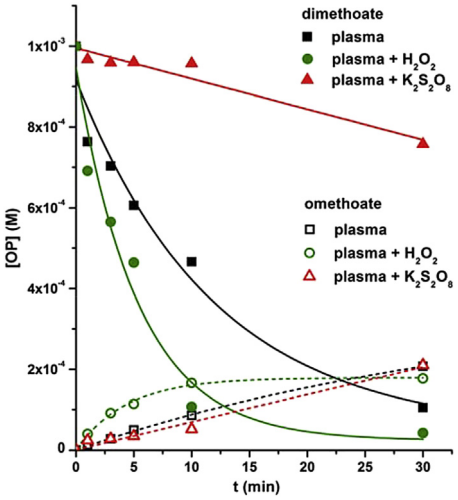

Fig. 5. The time dependence of the concentrations of DMT (full symbols, solid lines) and OMT (empty symbols, dashed lines) formed during the plasma needle treatment without free radical promoters (squares), in the presence of 0.09 M H_2O_2 (circles) and 0.09 M $K_2S_2O_8$ (triangles).

From the data presented in Fig. 5, it is obvious that the presence of free radical promoters affects the rate of DMT oxidation and degradation, but the effects are different for H_2O_2 and $K_2S_2O_8$. Degradation of DMT is more efficient in the presence of H_2O_2 comparing to regular plasma treatment of the same duration, resulting with the DMT concentration of only 4.20×10^{-5} M after 30 min of treatment. In contrast, the addition of $K_2S_2O_8$ only promoted the transformation of DMT to OMT. It has no distinct effect on the OMT degradation, since the concentration of formed OMT is equal to the concentration of degraded DMT (Fig. 5). In this sense, it can be concluded that $K_2S_2O_8$ selectively oxidize DMT to OMT, but it actually blocks DMT degradation pathways which do not go through OMT. Kinetic parameters for degradation of 1×10^{-3} M DMT solution and simultaneously OMT formation with or without 0.09M free radical promoters are presented in Table 2. It is obvious that the rate constant for DMT degradation (k_{obs}) is higher in the presence of H_2O_2 compared to plasma treatment without any free radical promoter. At the same time, when $K_2S_2O_8$ is added, k_{obs} significantly decreased. The rate constant for omethoate formation k_1 showed the same pattern. We conclude that the addition of H_2O_2 is favourable in the process of DMT degradation, unlike the addition of $K_2S_2O_8$. We assume that upon the addition of $K_2S_2O_8$ and generation of sulphate radicals reaction mixture becomes even more complex with a number of highly reactive species which could react mutually and in this way result with lower DMT degradation efficiency.

The obtained results showed that the addition of $K_2S_2O_8$ is not favourable in the process of dimethoate remediation. However, the addition of $K_2S_2O_8$ could potentially be used for DMT detection as DMT is selectively converted to OMT which can be effectively detected by enzymatic tests (Lazarevic-Pasti et al., 2010). This conclusion regarding the effect of $K_2S_2O_8$ are in harmony with recently published study by Aimer et al. (2019) The authors studied the degradation of DMT using heat-activated persulfate. The results showed that the disappearance of

Table 2
Kinetic parameters of 1×10^{-3} M dimethoate degradation and omethoate formation with or without 0.09M free radical promoters.

Free radical promoter	k_{obs} (min^{-1})	k_1 (min^{-1})
None	5.05×10^{-2}	3.94×10^{-2}
H_2O_2	18.59×10^{-2}	22.75×10^{-2}
$K_2S_2O_8$	1.25×10^{-7}	0.11×10^{-2}

the pesticide was quasi complete after 90 min for a 0.1 mM DMT solution, whereas only 15% was mineralized, thus confirming the selectivity of sulphate radical reactions with organics. Moreover, the toxicity assessment showed that the toxicity of the samples was enhanced during the reaction with persulphate. Based on the results presented here, we ascribe this effect to the OMT formation. This highlights that the use of the needle plasma for the treatment of water containing DMT can be used for both remediation and monitoring of DMT concentrations, as the transformations of DMT during the treatment can be successfully controlled.

3.3. Identification of intermediate products and possible degradation pathways

In order to clarify the degradation pathways of DMT, mass spectrometry was used to analyze the intermediates and products of DMT degradation during non-thermal plasma treatment. Considering possible low concentrations of intermediates, the sample with the highest concentration of DMT (1×10^{-3} M) was subjected to the MS analysis upon the treatment. MS spectra are provided in Supplementary Information. Schematic representation of the degradation mechanism, based on the indentified intermediates with characteristic masses, and DFT calculations is summarized in Fig. 6. The obtained results are in agreement with previously proposed mechanism of DMT degradation by dielectric barrier discharge plasma (Hu et al., 2013) and indicate that there could be four possible intermediates in this process beside omethoate. The main fragmentation ion at *m/z* of 213 corresponds to P=S from DMT converted to respective oxo-form P=O in OMT. Characteristic ions at *m/z* of 156, 126 and 110 are assigned to $[(CH_3O)_2(CH_3S)P(O)]^+$, $[(CH_3O)_2P(O)OH]^+$ and $[(CH_3O)_2P(OH)]^+$, respectively. Three characteristic ions with *m/z* of 156, 126 and 110 can be due to fragmentation of *O,O,S*-trimethyl phosphorothioate. Also, the ions with *m/z* of 156 and 126 can be related to $[(CH_3O)_3P(S)]^+$ and $[(CH_3O)_2P(SH)]^+$ from *O,O,O*-trimethyl thiophosphorothioate, along with $[CH_3O\text{-}P\text{-}H]+$ with the *m/z* ration of 63. Next intermediate product is identified as *O,O,S*-trimethyl thiophosphorothioate with the characteristic ions of $[(CH_3O)_2(CH_3S)P(S)]^+$, $[(CH_3O)_2P(S)]^+$ and $[(CH_3O)_2P(O)]^+$ at *m/z* of 172, 125 and 109. A peak at *m/z* of 105 corresponds to the molecular ion $[M]^+$ of *N*-methyl-2-sulfanylacetamide, while ions at *m/z* of 73 and 58 are related to the loss of HS^- and $HSCH_2^-$ fragments of this intermediate, respectively. Identified intermediates are in line with the DFT calculations, suggesting that P=S moiety of DMT and P1–S1–C1 parts of both DMT and OMT (Fig. 6) are susceptible to the attack by ·OH radical due to a high values of f_k^- corresponding to the S atoms of DMT and OMT, presenting the sites which readily react with electron acceptors. It is important to observe that upon the oxidation P=O moiety of OMT is not susceptible to the attack of electron acceptors and the degradation proceeds *via* cleavage of the P–S bond. Somewhat lower maximum value of f_k^- in OMT could explain its accumulation during the treatment with non-thermal plasma (Fig. 3) as the molecule becomes, in general, less sensitive to the attack of ·OH radical. To briefly summarize, DMT degradation starts with the attack of the ·OH on the P=S group and form P=O group of OMT. Then OMT is further converted in *N*-methyl-2-sulfanylacetamide and *O,O,S*-trimethyl phosphorothioate by cleavage of the P–S bond and the release of N-methyl acetamide groups. At the same time, DMT molecule gets transformed to *O,O,S*-trimethyl thiophosphorothioate and *O,O,O*-trimethyl thiophosphorothioate due to the cleavage of the S–C bond by · OH radical attack and further transformations along the degradation scheme. The formed intermediates can easily be transformed to small harmful molecules like PO_4^{3-}, H_2O and CO_2 (Fig. 6).

Table 3
The inhibition of the AChE activity in the presence of DMT (initial concentration ranging from 1×10^{-3} to 1×10^{-5} M) before and after the treatment with plasma for 30 or 120 min.

$[DMT]_0$ (M)	Treatment time (min)	AChE inhibition (% of control)
1×10^{-3}	0	50
	120	44
1×10^{-4}	0	15
	120	0
1×10^{-5}	0	5
	30[a]	0

[a] The treatment longer than 30 min for the lowest concentration of DMT was not necessary due to a fast degradation of both DMT and OMT (Fig. 3).

3.4. Toxicity assessment

We also analyzed the physiological effects of DMT samples in concentrations from 1×10^{-3} to 1×10^{-5} M before and after the treatment with plasma for 30 or 120 min with the Argon flow rate of 0.5 slm. As shown in Table 3, for the initial concentration of DMT used in

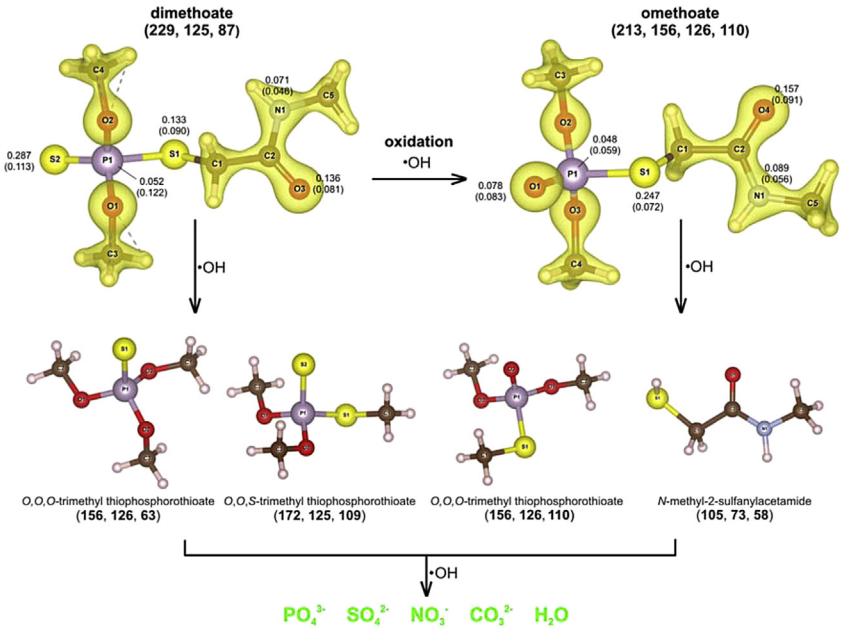

Fig. 6. Degradation pathways of DMT by non-thermal plasma. Top row – DFT optimized DMT and OMT molecules with 3D electron density maps (isosurface value 0.2 e Å−3) and Fukui indices of selected molecules (f_k^- and f_k^+ given in parentheses). In the second row the structures of the identified intermediates of DMT and OMT degradation by ·OH are given. Besides each structure we provide characteristic m/z values (parentheses, bold).

Table 4
The concentrations of remaining dimethoate ($[DMT]_r$) formed omethoate ($[OMT]_f$) and AChE inhibition in the tap water spiked with dimethoate with the initial concentration $[DMT]_0$ after the treatment with plasma for 30 min (At flow was 0.5 slm).

$[DMT]_0$ (M)	$[DMT]_r$ (M)	$[OMT]_f$ (M)	AChE inhibition (% of control), initial	AChE inhibition (% of control)
1×10^{-3}	8.54×10^{-4}	5.80×10^{-5}	50	33
1×10^{-4}	6.32×10^{-5}	1.13×10^{-5}	15	2
1×10^{-5}	6.22×10^{-7}	1.82×10^{-6}	5	0

plasma treatment experiments the AChE inhibition is induced, which translates into neurotoxic effects. However, after the treatment of DMT solutions with plasma, the sample with 1×10^{-3} M DMT showed lower AChE inhibition compared to that of the non-treated sample. Moreover, the samples with lower initial concentrations of DMT induced no AChE inhibition after the treatment. Hence, the toxicity of the DMT solutions was always decreased after the completion of the treatment with plasma.

3.5. Treatment of real samples with plasma

In order to demonstrate the feasibility of the proposed method in real samples, tap water spiked with DMT (1×10^{-3} to 1×10^{-5} M) was treated with plasma (0.5 slm) for 30 min. After that, the samples were analyzed *via* UPLC and the toxicity of the samples was estimated as described in Sections 2.3.1. and 2.4, respectively. The obtained data are presented in Table 4.

As expected, the concentration of DMT decreases monotonically during the treatment with plasma for all DMT concentrations tested. Moreover, the OMT concentration increases at the same time. However, the AChE inhibition is decreased in all tested samples upon the plasma treatment. This practically means that the toxicity of treated samples is reduced despite the increase in omethoate concentration, which is due to the decrease of DMT concentration. In this manner, toxicology studies confirmed that the proposed water treatment method is suitable for tap water remediation.

4. Conclusions

In the present work we demonstrate the use of non-thermal plasma needle for degradation of dimethoate in water. Considering that such approach has not been demonstrated so far, we present results regarding DMT degradation kinetics, possible degradation pathways, assess toxicity of treated water samples and confirm the feasibility of proposed method for treatment of real samples (tap water). The proposed treatment has excellent degradation efficiency, as it was found that 1×10^{-4} M dimethoate (batch volume 10 mL) can be fully degraded within 30 min using the Argon flow rate of 0.5 slm. Considering degradation products, the most important observation is formation of omethoate, rather toxic oxo-analogue of dimethoate. However, omethoate is also gradually removed upon the treatment. In spite omethoate formation, it is confirmed that the toxicity of the dimethoate solutions is decreased after the treatment with plasma in all the investigated cases. In order to investigate possible improvements of proposed method, addition of free radical promoters was also considered. Dimethoate removal is clearly improved with the addition of H_2O_2, which is likely due to additional formation of •OH radicals. In contrast, when $K_2S_2O_8$ is added dimethoate is selectively converted to its oxo-analogue omethoate. The feasibility of this treatment is demonstrated in real samples with unambiguous success. It should be emphasized that the proposed dimethoate degradation procedure is waste-free, unlike filtration methods, for example, and requires a low energy input for effective dimethoate removal. Therefore, this work provides a new method for treatment of contaminated water and has a great potential in detoxification of organophosphates in the environment.

Declarations of interest

None.

Acknowledgment

Authors acknowledge the support provided by the Serbian Ministry of Education, Science and Technological Development (project no. 172023). This work is a part of PhD thesis of T.M. under the supervision of S.L. and implemented within the projects III43007 (Serbian Ministry of Education, Science and Technological Development) and CGS50083 (Innovation Fund of the Republic of Serbia). This research did not receive any specific grant from funding agencies in the public, commercial, or not-for-profit sectors.

Appendix A. Supplementary data

Supplementary data to this article can be found online at https://doi.org/10.1016/j.jenvman.2019.05.143.

References

Aimer, Y., Benali, O., Groenen Serrano, K., 2019. Study of the degradation of an organophosphorus pesticide using electrogenerated hydroxyl radicals or heat-activated persulfate. Separ. Purif. Technol. 208, 27–33.
Armstrong, D.A., Huie, R.E., Lymar, S., Koppenol Willem, H., Merényi, G., Neta, P., Stanbury David, M., Steenken, S., Wardman, P., 2013. Standard electrode potentials involving radicals in aqueous solution: inorganic radicals. Bioinorg. React. Mech. 9, 59.
Badawy, M.I., Ghaly, M.Y., Gad-Allah, T.A., 2006. Advanced oxidation processes for the removal of organophosphorus pesticides from wastewater. Desalination 194 (1), 166–175.
Baxendale, J.H., Wilson, J.A., 1957. The photolysis of hydrogen peroxide at high light intensities. Trans. Faraday Soc. 53, 344–356.
Bruna, F., Pavlovic, I., Barriga, C., Cornejo, J., Ulibarri, M.A., 2006. Adsorption of pesticides carbetamide and metamitron on organohydrotalcite. Appl. Clay Sci. 33 (2), 116–124.
Chen, Y., Deng, P., Xie, P., Shang, R., Wang, Z., Wang, S., 2017. Heat-activated persulfate oxidation of methyl- and ethyl-parabens: effect, kinetics, and mechanism. Chemosphere 168, 1628–1636.
Colovic, M.B., Krstic, D.Z., Lazarevic-Pasti, T.D., Bondzic, A.M., Vasic, V.M., 2013. Acetylcholinesterase inhibitors: pharmacology and toxicology. Curr. Neuropharmacol. 11 (3), 315–335.
Cui, H.-F., Wu, W.-W., Li, M.-M., Song, X., Lv, Y., Zhang, T.-T., 2018. A highly stable acetylcholinesterase biosensor based on chitosan-TiO2-graphene nanocomposites for detection of organophosphate pesticides. Biosens. Bioelectron. 99, 223–229.
Ellman, G.L., Courtney, K.D., Andres jr., V., Featherstone, R.M., 1961. A new and rapid colorimetric determination of acetylcholinesterase activity. Biochem. Pharmacol. 7 (2), 88–95.
Fan, Y., Ji, Y., Kong, D., Lu, J., Zhou, Q., 2015. Kinetic and mechanistic investigations of the degradation of sulfamethazine in heat-activated persulfate oxidation process. J. Hazard Mater. 300, 39–47.
Foster, J., Sommers, B.S., Gucker, S.N., Blankson, I.M., Adamovsky, G., 2012. Perspectives on the interaction of plasmas with liquid water for water purification. IEEE Trans. Plasma Sci. 40 (5 PART 1), 1311–1323.
Giannozzi, P., Baroni, S., Bonini, N., Calandra, M., Car, R., Cavazzoni, C., Ceresoli, D., Chiarotti, G., Cococcioni, M., Dabo, I., Corso, A.D., Gironcoli, S., Fabris, S., Fratesi, G., Gebauer, R., Gerstmann, U., Gougoussis, C., Kokalj, A., Lazzeri, M., Martin-Samos, L., Marzari, N., Mauri, F., Mazzarello, R., Paolini, S., Pasquarello, A., Paulatto, L., Sbraccia, C., Scandolo, S., Sclauzero, G., Seitsonen, A., Smogunov, A., Umari, P., Wentzcovitch, R., 2009. QUANTUM ESPRESSO: a modular and open-source software project for quantum simulations of materials. J. Phys. Condens. Matter 21 (39), 395502.
Hu, Y., Bai, Y., Li, X., Chen, J., 2013. Application of dielectric barrier discharge plasma for degradation and pathways of dimethoate in aqueous solution. Separ. Purif. Technol. 120, 191–197.
Ji, Y., Dong, C., Kong, D., Lu, J., Zhou, Q., 2015. Heat-activated persulfate oxidation of

atrazine: implications for remediation of groundwater contaminated by herbicides. Chem. Eng. J. 263, 45–54.
Jiang, L., Li, H., Chen, J., Zhang, D., Cao, S., Ye, J., 2016. Combination of non-thermal plasma and biotrickling filter for chlorobenzene removal. J. Chem. Technol. Biotechnol. 91 (12), 3079–3087.
Kanazawa, S., Kawano, H., Watanabe, S., Furuki, T., Akamine, S., Ichiki, R., Ohkubo, T., Kocik, M., Mizeraczyk, J., 2011. Observation of OH radicals produced by pulsed discharges on the surface of a liquid. Plasma Sources Sci. Technol. 20 (3), 034010.
Lazarevic-Pasti, T., Anicijevic, V., Baljozovic, M., Anicijevic Vasic, D., Gutic, S., Vasic, V., Skorodumova, N.V., Pasti, I.A., 2018. The impact of the structure of graphene-based materials on the removal of organophosphorus pesticides from water. Environ. Sci.: Nano 5 (6), 1482–1494.
Lazarevic-Pasti, T., Leskovac, A., Momic, T., Petrovic, S., Vasic, V., 2017. Modulators of acetylcholinesterase activity: from alzheimer's disease to anti-cancer drugs. Curr. Med. Chem. 24 (30), 3283–3309.
Lazarevic-Pasti, T., Momic, T., Onjia, A., Vujisic, L., Vasic, V., 2010. Myeloperoxidase-mediated oxidation of organophosphorus pesticides as a pre-step in their determination by AChE based bioanalytical methods. Microchimica Acta 170 (3), 289–297.
Lazarevic-Pasti, T.D., Pasti, I.A., Jokic, B., Babic, B.M., Vasic, V.M., 2016. Heteroatom-doped mesoporous carbons as efficient adsorbents for removal of dimethoate and omethoate from water. RSC Adv. 6 (67), 62128–62139.
Lazovic, S., Puac, N., Maletic, D., Malovic, G., Petrovic, Z., Miletic, M., Pavlica, D., Jovanovic, M., Milenkovic, P., Bugarski, D., Mojsilovic, S., 2010. The effect of a plasma needle on bacteria in planktonic samples and on peripheral blood mesenchymal stem cells. New J. Phys. 12 (8), 21.
Leovac, A., Vasyukova, E., Ivancev-Tumbas, I., Uhl, W., Kragulj, M., Trickovic, J., Kerkez, D., Dalmacija, B., 2015. Sorption of atrazine, alachlor and trifluralin from water onto different geosorbents. RSC Adv. 5 (11), 8122–8133.
Li, G., Wang, B., Xu, W.Q., Han, Y., Sun, Q., 2018. Rapid TiO2/SBA-15 synthesis from ilmenite and use in photocatalytic degradation of dimethoate under simulated solar light. Dyes Pigments 155, 265–275.
Liu, X., Li, Y., Zhou, X., Luo, K., Hu, L., Liu, K., Bai, L., 2018. Photocatalytic degradation of dimethoate in Bok choy using cerium-doped nano titanium dioxide. PLoS One 13 (5), e0197560.
Liu, Y.H., Chung, Y.C., Xiong, Y., 2001. Purification and characterization of a dimethoate-degrading enzyme of Aspergillus Niger ZHY256, isolated from sewage. Appl. Environ. Microbiol. 67 (8), 3746–3749.
Lou, J., Lu, N., Li, J., Wang, T., Wu, Y., 2012. Remediation of chloramphenicol-contaminated soil by atmospheric pressure dielectric barrier discharge. Chem. Eng. J. 180, 99–105.
Maletic, D., Puac, N., Lazovic, S., Malovic, G., Gans, T., Schulz-von der Gathen, V., Petrovic, Z.L., 2012. Detection of atomic oxygen and nitrogen created in a radio-frequency-driven micro-scale atmospheric pressure plasma jet using mass spectrometry. Plasma Phys. Contr. Fusion 54 (12).
Manoli, K., Morrison, L.M., Sumarah, M.W., Nakhla, G., Ray, A.K., Sharma, V.K., 2018. Pharmaceuticals and Pesticides in Secondary Effluent Wastewater: Water Research Identification and enhanced removal by acid-activated ferrate(VI).
Matsushita, T., Morimoto, A., Kuriyama, T., Matsumoto, E., Matsui, Y., Shirasaki, N., Kondo, T., Takanashi, H., Kameya, T., 2018. Removals of pesticides and pesticide transformation products during drinking water treatment processes and their impact on mutagen formation potential after chlorination. Water Res. 138, 67–76.
Matzek, L.W., Carter, K.E., 2016. Activated persulfate for organic chemical degradation: a review. Chemosphere 151, 178–188.
Mirkovic, M.M., Pasti, T.D.L., Dosen, A.M., Cebela, M.Z., Rosic, A.A., Matovic, B.Z., Babic, B.M., 2016. Adsorption of malathion on mesoporous monetite obtained by mechanochemical treatment of brushite. RSC Adv. 6 (15), 12219–12225.
Momma, K., Izumi, F., 2008. VESTA: a three-dimensional visualization system for electronic and structural analysis. J. Appl. Crystallogr. 41 (3), 653–658.
Perdew, J.P., Burke, K., Ernzerhof, M., 1996. Generalized gradient approximation made simple. Phys. Rev. Lett. 77 (18), 3865–3868.
Połczyński, P., Jurczakowski, R., Grochala, W., 2013. Stabilization and strong oxidizing properties of Ag(ii) in a fluorine-free solvent. Chem. Commun. 49 (68), 7480–7482.
Puac, N., Miletic, M., Mojovic, M., Popovic-Bijelic, A., Vukovic, D., Milicic, B., Maletic, D., Lazovic, S., Malovic, G., Petrovic, Z., 2014. Sterilization of Bacteria Suspensions and Identification of Radicals Deposited during Plasma Treatment.
Samet, Y., Agengui, L., Abdelhedi, R., 2010. Anodic oxidation of chlorpyrifos in aqueous solution at lead dioxide electrodes. J. Electroanal. Chem. 650 (1), 152–158.
Savic, J.Z., Petrovic, S., Leskovac, A.R., Lazarevic-Pasti, T.D., Nastasijevic, B.J., Tanovic, B.B., Gasic, S.M., Vasic, V.M., 2019. UV-C light irradiation enhances toxic effects of chlorpyrifos and its formulations. Food Chem. 271, 469–478.
Schmid, R., Sapunov, V., 1982. Non-formal Kinetics in Search for Reaction Pathways. Verlag Chemie, Weinheim.
Valickova, M., Derco, J., Simovicova, K., 2013. Removal of selected pesticides by adsorption. Acta Chim. Slovaca 6, 25–28.
Vanysek, P., 2005. In: Lide, D.R. (Ed.), CRC Handbook of Chemistry and Physics. CRC Press, Boca Raton, FL.
Vela, N., Calína, M., Yáñez-GascónaIsabel, M.J., Garrido, I., Pérez-Lucasc, G., Fenoll, J., Navarro, S., 2018. Photocatalytic oxidation of six pesticides listed as endocrine disruptor chemicals from wastewater using two different TiO2 samples at pilot plant scale under sunlight irradiation. J. Photochem. Photobiol. A Chem. 353, 271–278.
WHO, 2011. Guidelines for Drinking-Water Quality, fourth ed. .
Wu, C., Linden, K.G., 2010. Phototransformation of selected organophosphorus pesticides: roles of hydroxyl and carbonate radicals. Water Res. 44 (12), 3585–3594.
Yamatake, A., Katayama, H., Yasuoka, K., Ishii, S., 2007. Water purification by atmospheric DC/pulsed plasmas inside bubbles in water. Int. J. Plasma Environ. Sci. Technol. 1 (1), 91–95.
Yang, H., Tezuka, M., 2011. Plasma-induced complete destruction of tetrachlorophenols in an aqueous solution. J. Phys. D Appl. Phys. 44 (15), 155203.
Yang, W., Mortier, W.J., 1986. The use of global and local molecular parameters for the analysis of the gas-phase basicity of amines. J. Am. Chem. Soc. 108 (19), 5708–5711.
Zaplotnik, R., Bišćan, M., Kregar, Z., Cvelbar, U., Mozetič, M., Milošević, S., 2015. Influence of a sample surface on single electrode atmospheric plasma jet parameters. Spectrochim. Acta B Atom Spectrosc. 103–104, 124–130.
Zhu, X., Li, B., Yang, J., Li, Y., Zhao, W., Shi, J., Gu, J., 2015. Effective adsorption and enhanced removal of organophosphorus pesticides from aqueous solution by Zr-based MOFs of uio-67. ACS Appl. Mater. Interfaces 7 (1), 223–231.